Aalborg Universitet

A New Method for Calculating the Error Term Used in 2D Feedback Control of Laser Forming

Thomsen, Anders Noel; Endelt, Benny Ørtoft; Kristiansen, Morten

Published in:
Physics Procedia

DOI (link to publication from Publisher):
10.1016/j.phpro.2017.08.003

Publication date:
2017

Document Version
Publisher's PDF, also known as Version of record

Available online at www.sciencedirect.com

ScienceDirect

Physics Procedia 89 (2017) 148 – 155

Physics Procedia

Nordic Laser Materials Processing Conference, NOLAMP_16, 22-24 August 2017, Aalborg University, Denmark

A new method for calculating the error term used in 2D feedback control of laser forming

Anders Noel Thomsen[a]*, Benny Endelt[a], Morten Kristiansen[a]

[a]Aalborg University, Department of Materials and Production, Fibigerstraede 16, Aalborg, 9220, Denmark

Abstract

Laser forming of sheet metal has the potential to add to the growing repertoire of laser processing. This is of particular interest for flexible manufacturing and rapid prototyping. A factor limiting the practical use is the planning of the process parameters, such as laser scan path, laser power, laser scan speed, laser spot size, dwell time, etc. This study presents a new method for calculating the error between the target shape and the current shape. The method is based on geometrical information and uses a projection of the second derivative of the target geometry unto the current geometry. By comparing the projected second derivative with the second derivative of the current geometry, the error can be calculated. Once the error has been found, a feedback control strategy can be used to update the process parameters. The new method entails that the error can be calculated without having to solve the large scale mechanical FEM as part of the planning process. This reduces the planning time and enables a simpler approach that, for the error calculation, is independent of material properties. The method is verified for a 2D feedback system for simple bends in sheet metal, using FEM simulations of the laser forming process.

Peer-review under responsibility of the scientific committee of the Nordic Laser Materials Processing Conference 2017

Keywords: Laser Forming, Automatic path planning

1. Introduction

Laser forming offers a potential of contactless shaping of metal components. The process is based on iteratively heating the surface of sheet metal with a laser beam to change the shape of the sheet. Utilizing a laser offers a versatile process, as the laser beam scan path combined with various process settings can be used to form sheet metal into a variety of shapes. Due to the versatility of the laser forming process, planning the optimal process

* Corresponding author. Tel.: +45 20763524.
E-mail address: ant@make.aau.dk

Peer-review under responsibility of the scientific committee of the Nordic Laser Materials Processing Conference 2017
doi:10.1016/j.phpro.2017.08.003

settings can be challenging. The laser forming process has been shown to cause a difference in bending angle in relation to laser power (Paunoiu et al. 2008), dwell time between scans and laser scan speed (Cheng & Yao 2001), number of laser beam scans in the same position and laser beam angle (Edwardson et al. 2006), etc. Two immediate issues apply to the planning of the laser forming process. One is planning the laser scan path to form the desired geometry. The other issue is ensuring the proper laser settings to achieve the desired bending angle.

Liu & Yao (2002) used a response surface methodology for optimization of the planning of 2D laser forming. In order to simplify the number of parameters, the authors placed each scan at a distance from each other so that they could be assumed to be independent. This poses a relatively large constraint that may also influence the smoothness of the formed shape. Kim & Na (2003) used geometric information to place laser scan points for 2D laser forming. The laser settings were determined based on experimental results managed in a database. The approach was shown to be able to approximate the target shape. However, the approach is based on an initial flat sheet, and cannot account for other initial shapes. In Kim & Na (2009), the same authors expanded the method for 3D but with the same limitations. Cheng & Yao (2004) used a genetic algorithm to plan the process of 2D laser forming for simple shapes. The approach is not considered to scale well for complex shapes. Liu et al. (2004) used the curvature to compute the required strains between the initial and target shape, using optimization. The strains were compared with a database to plan the process. A similar approach was undertaken by Liu & Yao (2005), who presented an approach to 3D that uses large deformation FEM to determine the strains required to achieve the target shape. Using the strain field removes the issue of an initial flat sheet, however the computational cost of calculating the strain field is increased. An issue of planning still persists as the methods are based on using a database of known bending behavior to determine the laser settings for the full forming procedure. This causes the method to be very dependent on the quality of the information in the database and the predictability of laser forming. Carlone et al. (2008) described an inverse analysis, comparing the target surface with deformed reference surfaces; however no verification using simulation or experimentation was shown. The predictability of laser forming is challenging, since the bending behavior is dependent on a variety of laser settings; therefore, another aspect should be considered.

The bending angle is increased in small increments per pass of the laser, which makes feedback control a relatively simple solution for determining the laser settings. Thomson & Pridham (1997) were the first to use 2D feedback control for laser forming. The authors used feedback control to achieve a certain bending angle while keeping the laser scan path constant. Kim & Na (2005) modified their approach for 2D feedback control. Their approach is based on updating the laser scan paths between runs. However, this did not solve the issue of using a database to determine the laser settings. By using geometric information, Kim & Na (2003) and Kim & Na (2005) achieved a faster solution compared to using large deformation FEM. However, some information may be lost if the simplified approach becomes too simplistic.

The authors of this work have attempted to walk the fine line by investigating the use of the curvature of the geometry as a measure of the bending. By comparing the curvature of the target shape with the curvature of the initial (or current in feedback) shape, the difference in curvature can be determined. The curvature can be manipulated by using a laser with the temperature gradient mechanism (TGM). This will eliminate several computations to determine the strains, which reduces total computation times. The present work describes the method of comparing the curvature of the target shape with the current shape. A simple controller has been designed to examine if the method can reduce the difference between the target shape and the current shape, see figure 1. Laser forming simulations are used to show the effect of the designed controller. The method is examined for three different shapes, see figure 2, a simple wide-bend, a bend requiring two narrower bends (two-bend), and the flattening of a pre-bend sheet.

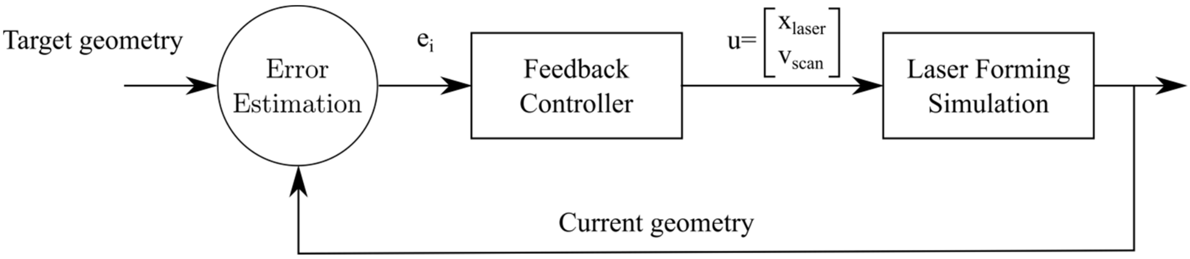

Figure 1. Block diagram of the approach. Each block is elaborated in section 2-4.

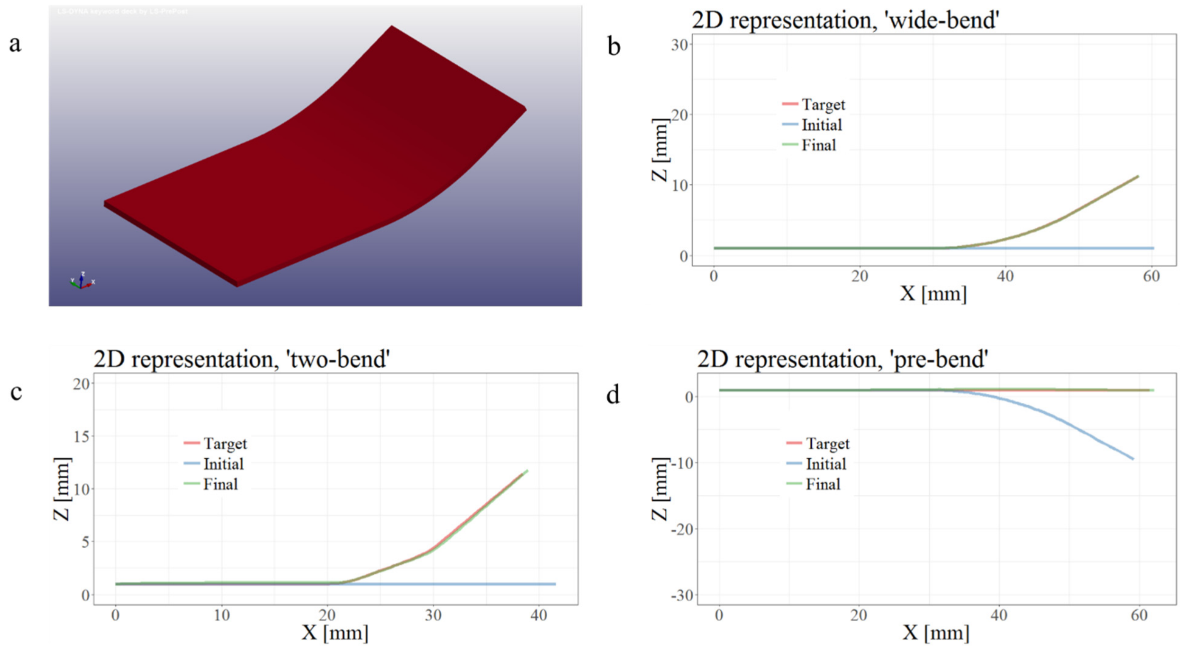

Figure 2. (a) The target wide-bend model in 3D. A 2D representation of the target shape can be seen in (b). (b)-(d) The three different target shapes with their corresponding initial and final achieved shapes, using the same proposed controller method.

2. Error estimation

The pseudo code used in the present work for error estimation can be seen below. The curvature is determined by differentiating the geometry twice with respect to x, using a central difference approach. The curvature is determined for the target and the current geometry. A projection of the curvature is made from the target to the current geometry. The projection is performed by placing N equally spaced nodes on the target geometry and N equally spaced nodes on the current geometry. It may be assumed that each node *i* corresponds to the same relative position on both target and current geometry. An illustration of the principle can be seen in figure 3. Ideally, the middle line, see figure 3, could be used for the projection as there is no contraction or stretching during pure bending. However, it is not practical to use the middle line in an actual experimental setup. Therefore, the topline, see figure 3, is used in the present work, which means that the projection is dependent on the thickness of the plate. For thin sheets, the thickness dependency is believed to be negligible. Once the projection is complete, the curvature of the current geometry can be subtracted from the curvature of the target geometry, thereby attaining the difference in curvature.

An issue when using the second derivative is noise handling. While simple in principle, differentiation is notorious as regards noise sensitivity. Therefore, a strategy for handling noise may be required. The strategy must not introduce a phase shift as this will shift the positions of the relevant peaks and thereby the position of the laser. A simple averaging filter is used in the present work, as this does not introduce a phase shift. The filter is based on an average of five points, and the same filter is applied three times to reduce noise.

Pseudo code – Error estimation:

1. Distribute *N* nodes over the target geometry based on equal spacing between nodes, see figure 3.
2. The target geometry is differentiated twice at each of the *N* nodes with respect to x.
3. The current geometry is established.
4. Distribute *N* nodes over the current geometry based on equal spacing between nodes, see figure 3.
5. The current geometry is differentiated twice at each of the *N* nodes with respect to x.
6. The second derivative of the current geometry is filtered 3 times using the same moving average filter with an average based on 5 points.
7. The error (e_i) at each Node (i) in the current geometry is calculated using equation (1), where the indexes *ti* and *ci* relate to the i'th node for the target and current geometry respectively.
$$e_i = \frac{d^2 y_{ti}}{dx^2} - \frac{d^2 y_{ci}}{dx^2} \quad (1)$$
8. The error term (e_i) is passed on to the feedback controller.

It is worth noting that the first two steps involving the target geometry only have to be completed the first time, as the calculations can be reused for subsequent iterations.

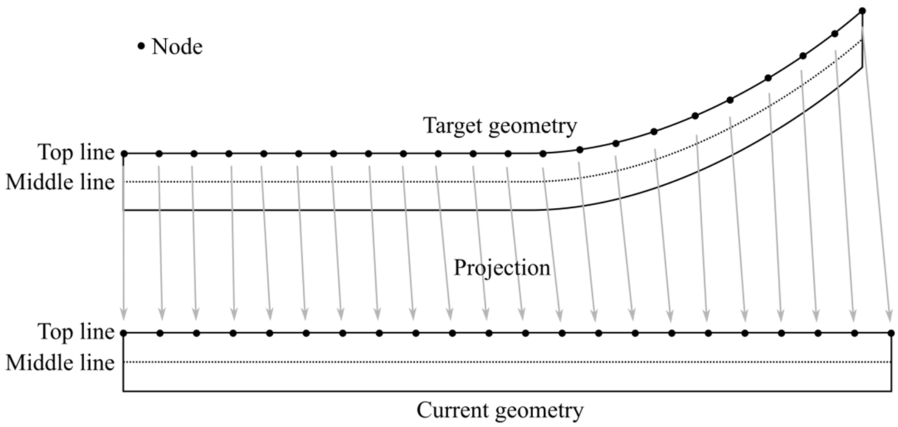

Figure 3. Projection from target geometry to the current geometry.

The initial error estimation for the wide bend model can be seen in figure 4. As the curvature is based on differentiation with respect to x, a constant bend will not yield a constant error term. This is not an issue with the present setup as the loop is updated often, and the curvature is always calculated the same way. As the entire bend will begin to form, the response will be greater in this area, and the error term will be reduced correspondingly. However, this could be a problem if greater planning of the process was involved. A possible solution to this is to use a local coordinate system that is invariant to the orientation of the shape, which will yield the theoretical line in figure 4. The small peaks in figure 4 derive from the mesh in LS-Dyna, where the model was created.

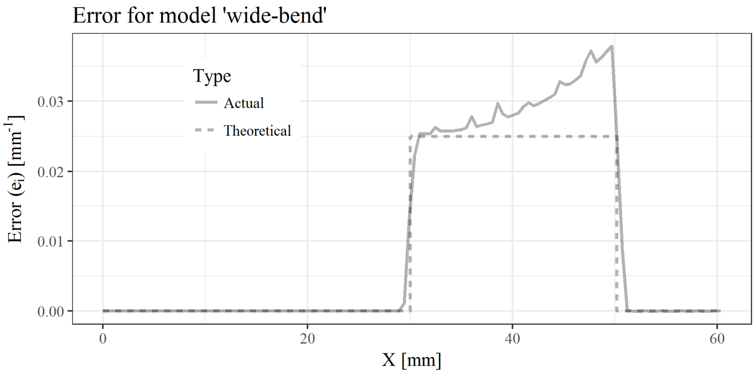

Figure 4. The error for the wide bend model. The dashed line represents the theoretical line achievable by using a local coordinate system.

3. Feedback control

The error estimation is a measure of the difference in curvature at each point. The error estimation allows the use of different strategies for conducting the feedback control. The present work uses the same approach for all shapes. This approach utilizes the laser forming process, which affects a small area along the x-axis. The error (e_i) is integrated to E_i based on numerical integration of the eleven nearest points as in equation (2). The number of points used should be correlated to the area of effect by the laser. Eleven points were chosen empirically in the present work. The max(E_i) is found along with the corresponding x position of E_i. The x position is used as the position of the laser along the x-axis (x_{laser}), and the value of E_i is used to determine the laser scan speed. The purpose of this approach is to avoid heating the edge between the positions in which e_i is zero and non-zero to avoid overshooting. The pseudo code can be seen in the following, and Table 1 contains the used controller parameters. The feedback loop is run until an end value (ε) for E_i is reached, where ε is a preset value to avoid overshoot. Overshoot is a problem, as the forming cannot be reversed. Therefore, it is better to stop in advance than to attempt to reduce the error to zero.

Pseudo code – Feedback control:

9. Find i for the maximum value of E_i where E_i can be determined by equation (2).

$$E_i = \left(x_{i+5} - x_{i-5}\right)\sum_{j=i-5}^{i+5}\frac{e_j}{11} \tag{2}$$

10. If $E_i < \varepsilon$ then stop the program, else continue.
11. The laser position (x_{laser}) is set to x_i.
12. The laser scan speed is set to v_{scan} following equation (3)

$$v_{scan} = v_{\max} - kE_i \tag{3}$$

13. If $v_{scan} < v_{min}$ set $v_{scan} = v_{min}$
14. v_{scan} and x_{laser} is sent to the laser forming setup.
15. Laser forming is simulated using Ls-Dyna.

Table 1. Controller parameters

Parameter	Description	Value	Unit
N	Number of nodes	120	
ε	Stop value for the feedback loop	0.01	
v_{max}	Maximum scan speed	4500	mm/min
v_{min}	Minimum scan speed	3000	mm/min
k	Gain for the feedback controller	2	10^4 mm^2/min

4. Laser forming simulation

The Laser forming simulations are made using Ls-Dyna as an implicit coupled thermal mechanical analysis. It should be noted that the purpose of the simulations is not to give an exact representation of the process, but rather to show similar bending behavior in order to test the error estimation method. The laser heat is implemented as a heat flux with a Gaussian distribution, which means that no penetration of the surface takes place. The laser heat is implemented to reflect a vertical laser beam. For non-horizontal shapes, this will cause a distortion from a round heat input as commented by Edwardson et al. (2006). The boundary conditions used are identical for all geometries and include mechanical clamping at one end, convection on all surfaces, and the setting of the far end (the clamped end) to a constant temperature of 293 K. The time steps for both the mechanical and thermal solvers are automatically calculated, but are not synchronized to reduce total computation time. The mesh for the wide bend is shown in figure 5. Similar meshes are used for the pre-bend and two-bend models. Laser forming is an iterative process; therefore, the simulations are based on continuously updated models. It is assumed that full cooling occurs between runs, i.e. the model always starts at a temperature of 293 K.

Figure 5 shows a mesh for the wide-bend initial geometry. Similar meshes are made for the other shapes, with a refined mesh in the zone in which the laser is used and a coarser mesh in the remaining part. The shapes are all 30 mm wide (y direction) and have a thickness of 1 mm (z direction). It is worth noting that the conversion to the 2D representation shown in figure 5 is conducted by exporting the nodal coordinates of the top edge at y = 30 mm and z = 1 mm. This is to avoid some of the edge effects, which may cause the center of the plate to bend inwards. There are several ways of reducing edge effects, which must be considered when examining 3D problems, Shen et al. (2010); however, these are not included in the present work.

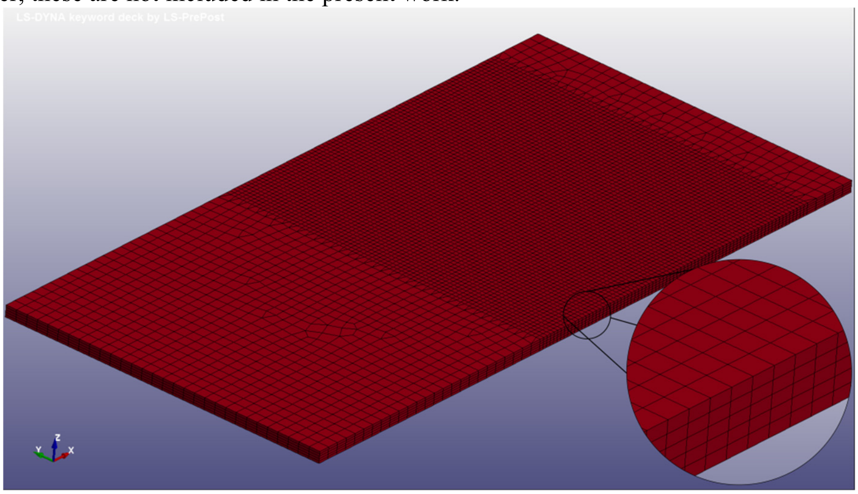

Figure 5. The wide-bend initial geometry. A refined mesh is used in the zone with direct heat from the laser.

5. Results and discussion

The final achieved shape with the target shape for each of the three shapes can be seen in figure 2. The corresponding sum of squared residuals (SSR) can be seen in figure 6a-c, while figure 6d-f shows the evolution of max(E_i) for each iteration. It can be seen in figure 6d-f that only the wide-bend model achieved the target ε value of 0.01. The other two models were stopped after 175 iterations. However, all three models are converging towards the target shape. While the pre-bend and two-bend models both begin to diverge, it appears that both models are below a SSR of 1 mm^2 at some point. It is therefore believed that the divergence is an issue of proper controller design rather than an issue relating to error estimation. This is considering that the wide-bend model that achieves a SSR of 0.02 mm^2 after 82 iterations, which shows that it can be a viable method through proper adjustments to the controller.

The lowest SSR was found for each model of 0.02 mm^2, 0.7 mm^2 and 0.6 mm^2 for the wide-bend, the two-bend, and the pre-bend models respectively. While the two-bend model shows the most noticeable signs of divergence, this also applies to the pre-bend model. A reason for this could be the choice of integration points for E_i. The controller was designed in the present work by empirically choosing appropriate parameters for the gain (k), the number of integration points in E_i and the number of nodes used. The number of integration points used for E_i is dependent on the number of nodes N, as the number of nodes affects the distance between each node. This also applies to the total length of the shape. A simple approach is to make a trial run and estimate how many nodes are affected by a single scan of the laser, and subsequently using this to estimate the number of integration points to be used.

The total forming time was not part of the present study, as the total processing time can be further reduced by changing the controller design. The designed feedback loop is updated after each laser scan, yet the total processing time can be reduced by planning several laser scans in each loop, thus saving time spent on measuring the geometry. A consideration in planning ahead is that a wrongful laser scan is difficult to undo. Cheng & Yao (2001) achieved a bend of 0.5-3 per pass of the laser. The risk of melting the surface causes limitations to the amount of bending per pass. Therefore, a strategy to ensure a higher degree of planning in the early stages to approximate the shape and switch to updating the loop more often when precision is required may be a solution.

The issues with the controller merit more work. The solutions may not be applicable in a 3D scenario. Therefore, the next step is to convert the method into 3D.

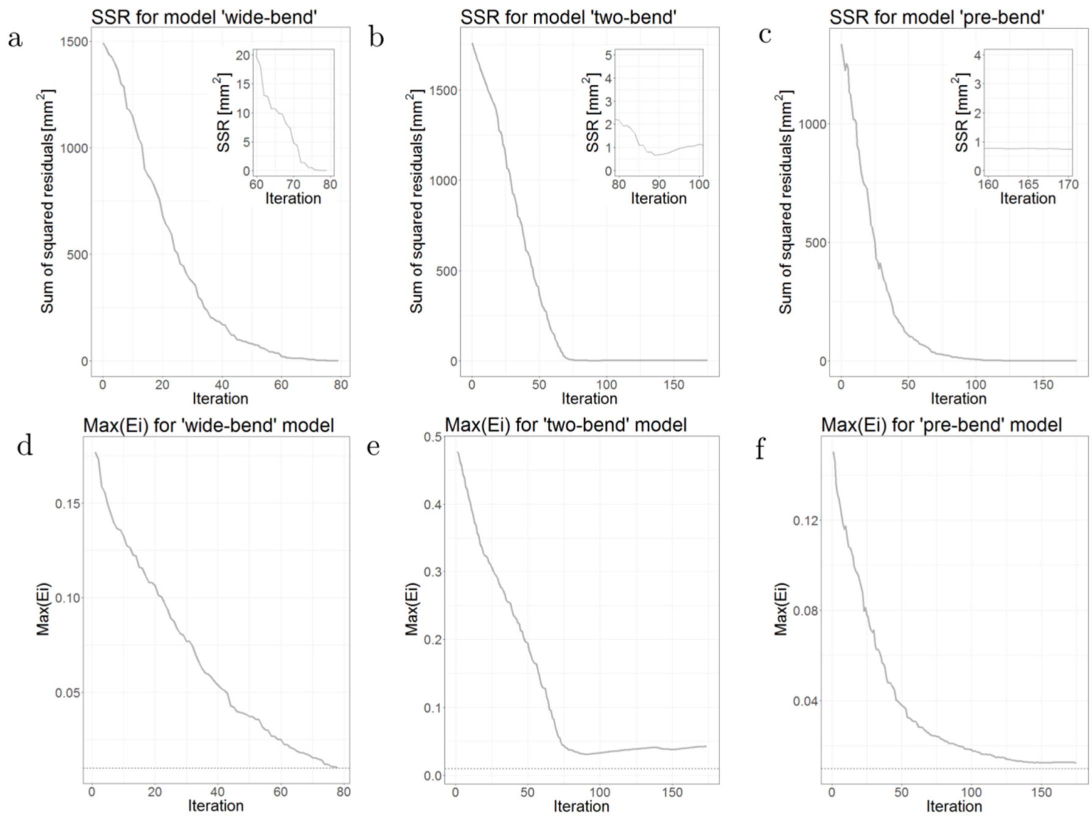

Figure 6. SSR and max(E_i) as a function of iterations. (a) SSR for wide-bend. The zoomed area shows the convergence towards the target shape (b) SSR for the two-bend. The zoomed area shows a small divergence from the target shape. (c) SSR for pre-bend. The zoomed area shows a steady state error. (d) max(E_i) for wide-bend. (e) max(E_i) for two-bend. (f) max(E_i) for pre-bend.

The primary benefit of the developed method is reduced computational time through simplifications. This benefit is gained by assumptions, which may disrupt the method if not understood.

- The method only accounts for pure bending which can be achieved with the TGM.
- The projection based on the top line is dependent on the use of thin sheets as the difference between the top line and middle line will be greater for thicker sheets.
- The method cannot account for differences in dimensions in the initial sheets compared to the final sheets, for example, if the initial sheet is twice as long as the target sheet. If sheets of different dimensions are used, it is expected that the final shape will be a scaled and possibly skewed version of the target shape.

6. Conclusion

A simplified method for evaluating the difference between a target shape and the current shape using the curvature has been developed. A simple controller was designed to test the method. Laser forming simulations were used to show that the controller was able to reduce the difference between a target shape and a current shape. The curvature has been shown to be a viable option for planning the laser scan path for 2D laser forming bends. Three different models were made to evaluate the method, and an SSR of 0.02 mm^2 was achieved for the wide-bend shape. The other two models showed an SSR of 0.7 mm^2 and 0.6 mm^2 for the two-bend and the pre-bend model respectively before the controller diverged before meeting the required end value. While focus could be placed on improving the controller, the next step should be to expand the method to 3D error estimation.

Acknowledgements

Support for this project under work package 3 by the Manufacturing Academy Denmark (Made) is gratefully acknowledged. Equipment used for this project was supported by the Poul Due Jensen Foundation.

References

Carlone, P., Palazzo, G.S. & Pasquino, R., 2008. Inverse analysis of the laser forming process by computational modelling and methods. Computers and Mathematics with Applications, 55(9), pp.2018–2032.

Cheng, J. & Yao, Y.L., 2001. Cooling effects in multiscan laser forming. Journal of Manufacturing Processes, 3(1), pp.60–72.

Cheng, J.G. & Yao, Y.L., 2004. Process synthesis of laser forming by genetic algorithm. International Journal of Machine Tools and Manufacture, 44(15), pp.1619–1628.

Edwardson, S.P. et al., 2006. Geometrical influences on multi-pass laser forming. Journal of Physics D: Applied Physics, 39, pp.382–389.

Kim, J. & Na, S.J., 2003. Development of irradiation strategies for free curve laser forming. Optics & Laser Technology, 35(8), pp.605–611.

Kim, J. & Na, S.J., 2005. Feedback control for 2D free curve laser forming. Optics & Laser Technology, 37, pp.139–146.

Kim, J. & Na, S.J., 2009. 3D laser-forming strategies for sheet metal by geometrical information. Optics & Laser Technology, 41, pp.843–852.

Liu, C. & Yao, Y.L., 2005. FEM-based process design for laser forming of doubly curved shapes. Journal of Manufacturing Processes, 7(2), pp.109–121.

Liu, C. & Yao, Y.L., 2002. Optimal and Robust Design of the Laser Forming Process. Journal of Manufacturing Processes, 4(2), pp.52–66.

Liu, C., Yao, Y.L. & Srinivasan, V., 2004. Optimal Process Planning for Laser Forming of Doubly Curved Shapes. Journal of Manufacturing Science and Engineering, 126(1), p.1.

Paunoiu, V. et al., 2008. Laser Bending of Stainless Steel Sheet Metals. Journal of Materials, pp.1371–1374.

Shen, H., Hu, J. & Yao, Z., 2010. Analysis and control of edge effects in laser bending. Optics and Lasers in Engineering, 48(3), pp.305–315.

Thomson, G. & Pridham, M., 1997. A feedback control system for laser forming. Mechatronics, 7(97), pp.429–441.